Red vs. blue quasars

Klindt et. al.

Durham University

July 2019

Abstract

ABSTRACT

A minority of the optically selected quasar population are red at optical wavelengths due to the presence of dust along the line of sight. A key focus of many red quasar studies is to understand their relationship with the overall quasar population: are they blue quasars observed at a (slight) inclination angle or do they represent a transitional phase in the evolution of quasars? Identifying fundamental differences between red and blue quasars is key to discriminate between these two paradigms. To robustly explore this, we have uniformly selected quasars from the Sloan Digital Sky Survey with mid-infrared counterparts, carefully controlling for luminosity and redshift effects. We take a novel approach to distinguish between colour-selected quasars in the redshift range of $0.2 < z < 2.4$ by constructing redshift-sensitive $g^* - i^*$ colour cuts. From cross-matching this sample to the Faint Images of the Radio Sky at Twenty-centimeters (FIRST) survey, we have found a factor ≈ 3 larger fraction of radio-detected red quasars with respect to that of blue quasars. Through a visual inspection of the FIRST images and an assessment of the radio luminosities (rest-frame $L_{1.4\,\mathrm{GHz}}$ and $L_{1.4\,\mathrm{GHz}}/L_{6\,\mu\mathrm{m}}$), we find that the radio-detection excess for red quasars is primarily due to compact and radio-faint systems (around the radio-quiet – radio-loud threshold). We show that our results rule out orientation as the origin for the differences between red and blue quasars and argue that they provide broad agreement with an evolutionary model.

What we know about QSOs:

- Dust in the torus, heated by the accretion disk, emits thermally at MIR: 5-40 μm, drops off steeply to FIR 40-500 μm
- 5-10% of optically detected QSOs are powerful at radio.
- Broad emission lines+power-law continuum: rQSOs with redder continuum challenged this

Uncertain nature of rQSOs

1. Dust reddening of accretion disc emission
2. (or) The excess of flux at longer wavelengths: synchrotron or host G contamination?
3. (or) Intrinsic red continuum: accretion disk difference and/or Eddingthon ratio difference compared to normal quasars?

Orientation or Evolution?

- Difference of nearby obscured/unobscured AGNs: explained by dusty torus viewing angle
- Rare red quasars: Transition between dusty SF and clearing of LOS by outflow/feedback.

Challenge in studying rQSOs

- Broad range of selection approach: optical-NIR-MIR colour criteria, point-source morphologies, and bright radio emission
- No uniform blue control sample in most studies: z, M_{BH}, L, Edd. ratio

Sample selection flowchart

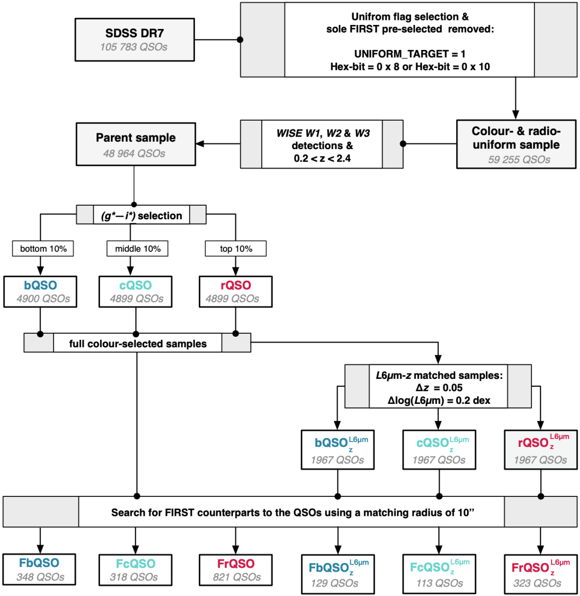

Sample statistics

Sample (1)	N_{z1-z4} (2)	N_{z1} (3)	N_{z2} (4)	N_{z3} (5)	N_{z4} (6)
Parent QSO	48 964	5402	6021	18 286	19 255
Colour-selected QSO samples					
bQSOs	4900	535	613	1822	1923
cQSOs	4899	543	597	1826	1929
rQSOs	4899	545	590	1833	1930
FbQSOs	348	62	71	110	105
FcQSOs	318	52	48	121	97
FrQSOs	821	99	127	298	297
Matched $L_{6\mu m}$–z QSO samples					
$\mathrm{bQSO}_z^{L_{6\mu m}}$	1967	159	256	781	771
$\mathrm{cQSO}_z^{L_{6\mu m}}$	1967	161	252	780	773
$\mathrm{rQSO}_z^{L_{6\mu m}}$	1967	161	252	781	772
$\mathrm{FbQSO}_z^{L_{6\mu m}}$	129	12	32	44	41
$\mathrm{FcQSO}_z^{L_{6\mu m}}$	113	13	20	43	37
$\mathrm{FrQSO}_z^{L_{6\mu m}}$	323	39	51	121	112

Red-shift evolution sensitive sample selection

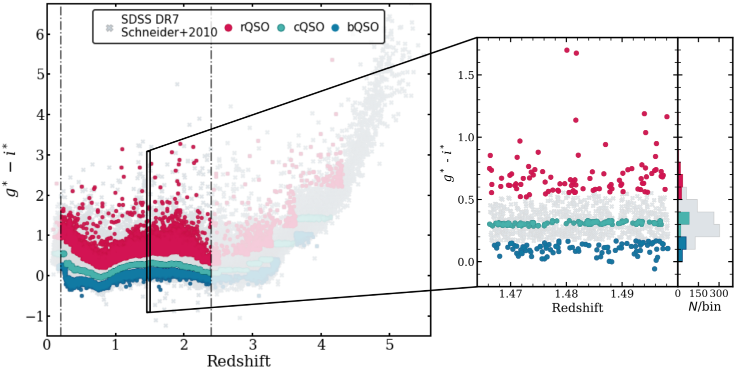

rQSOs are red in both $g^* - i^*$ and $u^* - r^*$

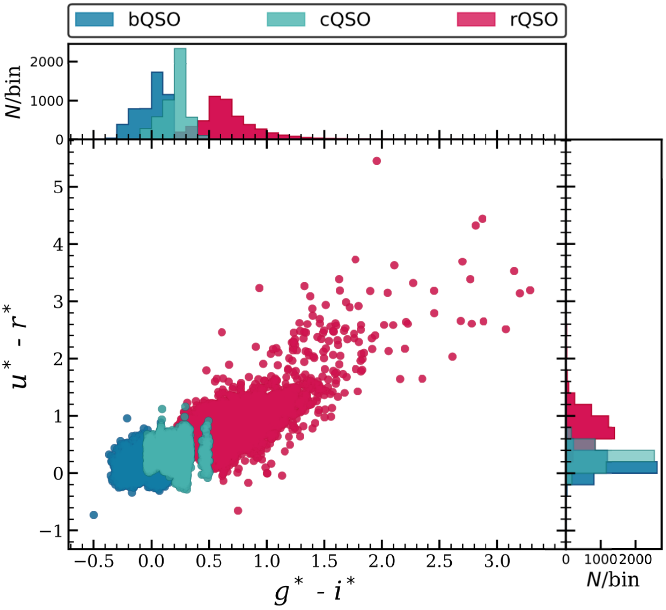

Dust-extinction (SMC, $N_H > 2.8 \times 10^{28}$ cm^{-2})

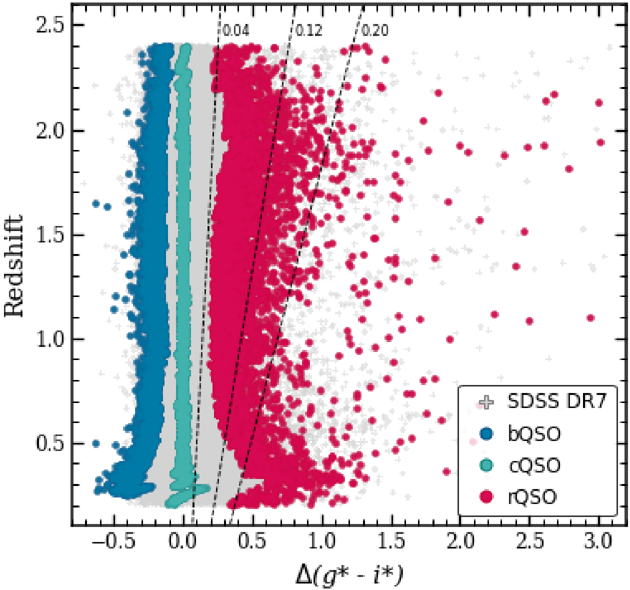

AGN Wedge: MIR/FIR → AGN/SF

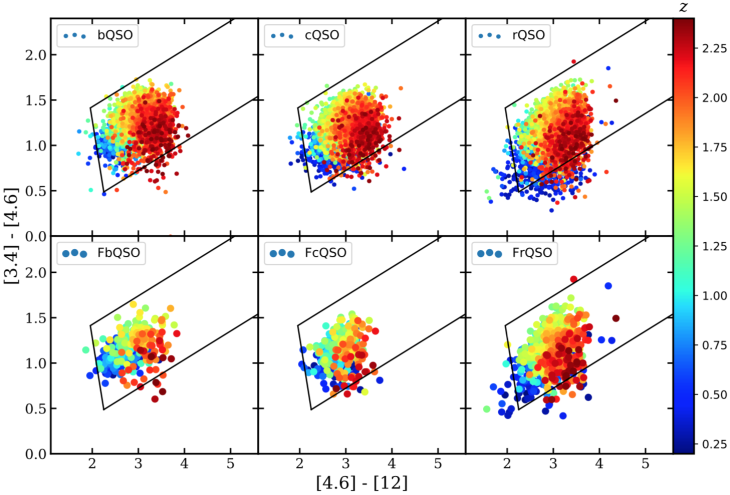

Number and percentage outside AGN wedge

Sample	Nu. outside	Percentage outside		
		$0.2 < z < 2.4$	$z < 1.5$	$z > 1.5$
Colour-selected quasars				
bQSO	56	1%	0.3%	0.8%
cQSO	82	2%	0.8%	0.9%
rQSO	305	6%	4%	2%
FIRST- detected quasars				
FbQSO	8	2%	0.9%	1%
FcQSO	9	3%	1%	2%
FrQSO	43	5%	3%	2%

$\text{Lum}_{6\mu m}$ vs. z

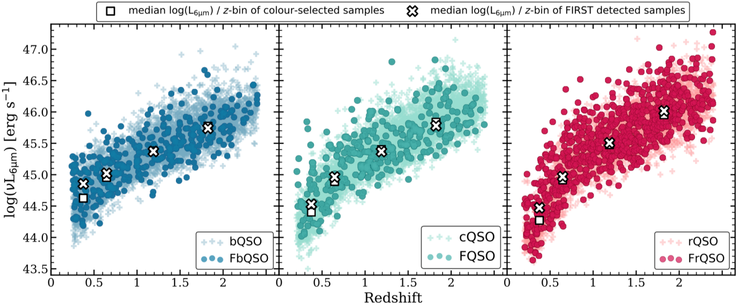

Luminosity distribution

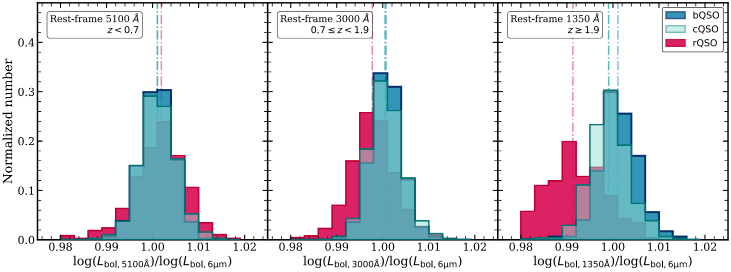

Radio detection

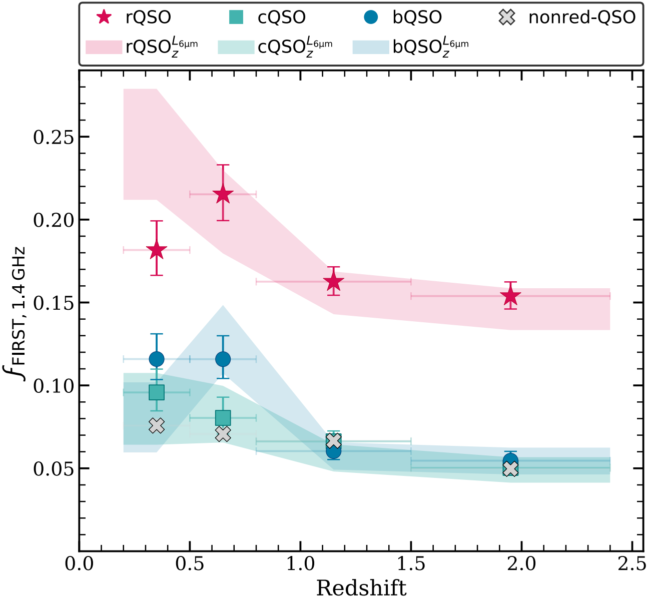

FIRST detection percentage

Redshift	FIRST-detected percentage (%)			
	bQSO	cQSO	rQSO	non-red QSO
$0.2 < z < 0.5$	$11.6^{+1.5}_{-1.2}$	$9.6^{+1.4}_{-1.1}$	$18.2^{+1.8}_{-1.5}$	$7.1^{+0.4}_{-0.3}$
$0.5 < z < 0.8$	$11.6^{+1.4}_{-1.2}$	$8.0^{+1.3}_{-0.9}$	$21.5^{+1.8}_{-1.6}$	$6.7^{+0.2}_{-0.2}$
$0.8 < z < 1.5$	$6.0^{+0.6}_{-0.5}$	$6.6^{+0.6}_{-0.5}$	$16.3^{+0.9}_{-0.8}$	$5.0^{+0.2}_{-0.2}$
$1.5 < z < 2.4$	$5.5^{+0.6}_{-0.5}$	$5.0^{+0.5}_{-0.5}$	$15.4^{+0.8}_{-0.8}$	$7.6^{+0.4}_{-0.4}$

FIRST radio detection in i-g quantiles

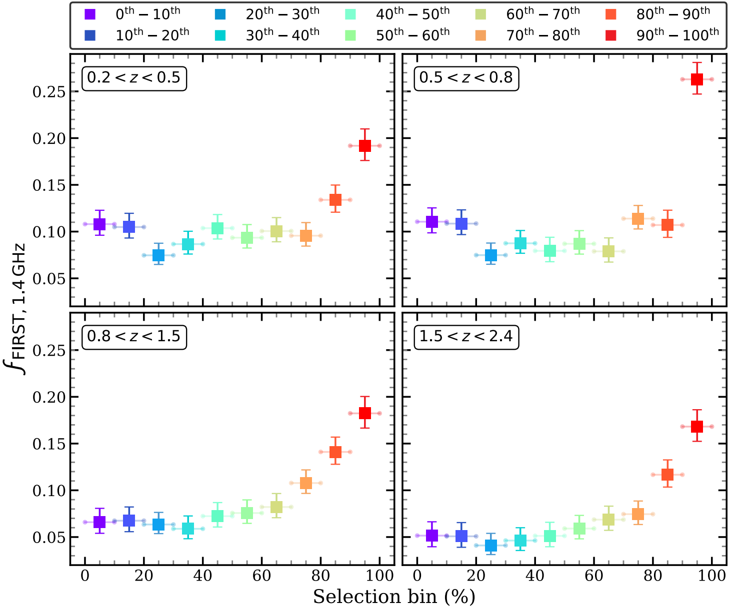

Radio morphology Classificaion

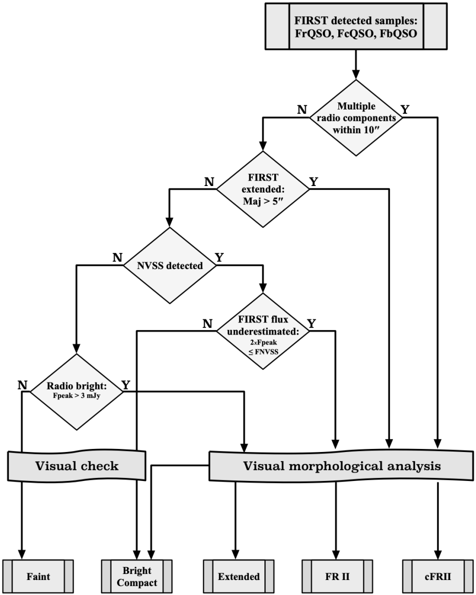

Radio Morphology Classes

Table 4. The radio morphology classes used to classify the FIRST images for the radio-detected quasars.

Classification	Description
Faint	Sources detected close to the FIRST detection threshold with peak fluxes of $F_{\mathrm{peak}} < 3$ mJy.
Compact	Sources that are point-like with non-extended emission (fitted major axes < 5 arcsec).
Extended	Single radio sources that are extended. This class includes FR I-like systems where both lobes are fainter than the core; $F_{\mathrm{lobe}} < F_{\mathrm{peak}}$.
FR II-like	Double lobed systems with approximately the same brightness and offset from QSO position. At least one lobe should be brighter than than QSO core ($F_{\mathrm{lobe}} > F_{\mathrm{peak}}$).
Compact FR II	FR II-like systems on small scales, i.e within the 10 arcsce radius circle (which corresponds to a projected size of ~ 85 kpc at $z = 1.5$).

NVSS vs. FIRST flux at 1.4 GH

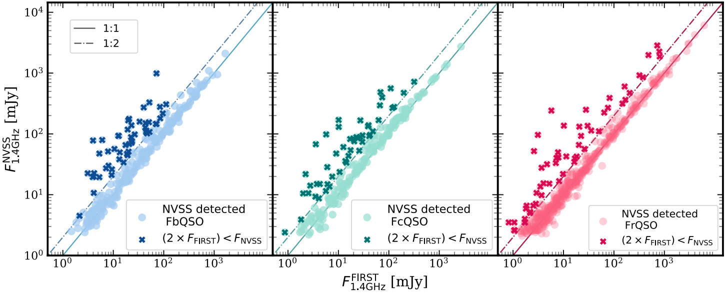

Radio Morphology and Color

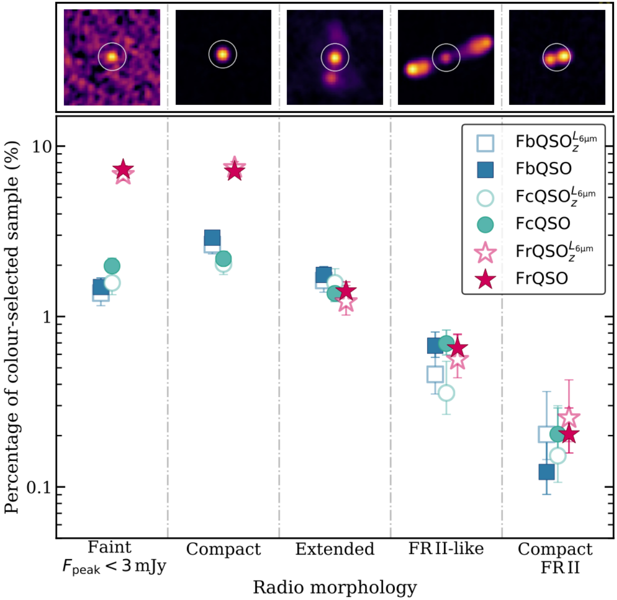

Quasars in each morphology classes

Classification	bQSO	cQSO	rQSO
The number of quasars in each class			
Faint	73	97	357
Compact	142	107	348
Extended	86	67	69
FR II-like	33	34	32
Compact FR II	6	10	10
The percentage in each class (see Fig. 12)			
	(%)	(%)	(%)
Faint	$1.49^{+0.193}_{-0.153}$	$1.98^{+0.218}_{-0.179}$	$7.287^{+0.387}_{-0.352}$
Compact	$2.898^{+0.258}_{-0.22}$	$2.184^{+0.228}_{-0.189}$	$7.103^{+0.383}_{-0.348}$
Extended	$1.755^{+0.207}_{-0.168}$	$1.368^{+0.186}_{-0.146}$	$1.408^{+0.188}_{-0.148}$
FR II-like	$0.673^{+0.137}_{-0.097}$	$0.694^{+0.139}_{-0.099}$	$0.653^{+0.136}_{-0.096}$
Compact FR II	$0.122^{+0.073}_{-0.032}$	$0.204^{+0.086}_{-0.046}$	$0.204^{+0.086}_{-0.046}$

Radio loudness of FbQSOs, FcQSOs, and FrQSOs

R	Sample	Faint	Compact	Extended
−4.75	FbQSO	53	14	7
	FcQSO	84	16	11
	FrQSO	321	63	13
−3.75	FbQSO	17	26	29
	FcQSO	11	25	16
	FrQSO	33	108	27
−3.25	FbQSO	2	41	39
	FcQSO	0	26	34
	FrQSO	0	85	27
−2.25	FbQSO	0	61	50
	FcQSO	0	40	50
	FrQSO	0	87	43

Radio luminosity at 1.4 GHz vs. z for FbQSO,FcQSO,and FrQSO

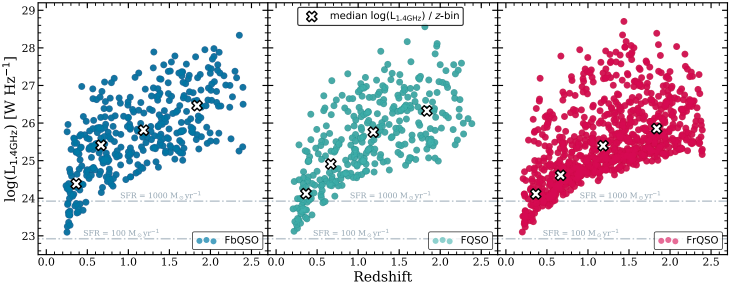

Relative fraction of FIRST-detected BALQSOs compared to FcQSOs as a function of R

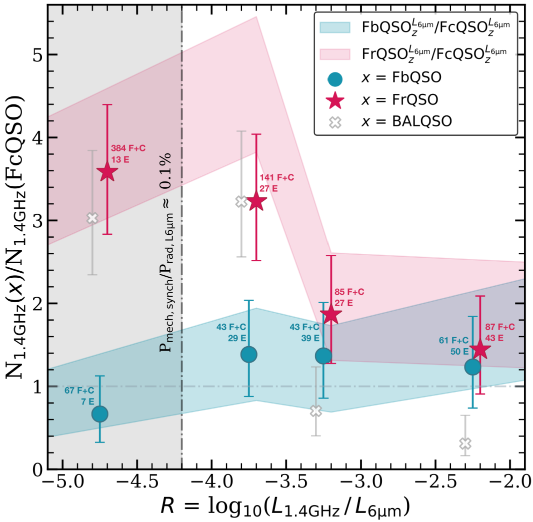

Estimated bolometric luminosity (Lbol, 6μm) vs. FWHM for the b,c,rQSO$_z^{L_{6\mu m}}$